Published in final edited form as:
J Biomater Tissue Eng. 2011 June 1; 1(1): . doi:10.1166/jbt.2011.1005.

Thermoresponsive Nanocomposite Hydrogels: Transparency, Rapid Deswelling and Cell Release

Yaping Hou[1], **Ruochong Fei**[1], **Jonathan C. Burkes**[1], **Shin Duk Lee**[1], **Dany Munoz-Pinto**[2], **Mariah S. Hahn**[2], and **Melissa A. Grunlan**[1,*]

[1]Department of Biomedical Engineering, Materials Science and Engineering Program, Texas A&M University, College Station, 77843 TX, USA

[2]Department of Chemical Engineering, Texas A&M University, College Station, 77843 TX, USA

Abstract

Thermal modulation reversibly switches poly(*N*-isopropylacrylamide) (PNIPAAm) hydrogels between a water-swollen and a deswollen state which is useful for a variety of biomedical applications. The utility and efficiency of PNIPAAm hydrogels requires tailoring their rate of deswelling/reswelling, mechanical properties and/or optical clarity. In the current work, we prepared novel thermoresponsive nanocomposite hydrogels comprised of a PNIPAAm hydrogel matrix and polysiloxane colloidal nanoparticles (~54 nm ave. diameter) via *in situ* photopolymerization of aqueous solutions of NIPAAm monomer, *N*,*N*′-methylenebisacrylamide (BIS, crosslinker), photoinitiator and 0.5–4.0 wt% polysiloxane nanoparticles (wt% solids of nanoparticles with respect to NIPAAm weight) at ~7 °C. At these nanoparticle concentrations, the nanocomposite hydrogels were more optically transparent versus those prepared with analogous larger nanoparticles (~219 nm ave. diameter). The volume phase transition temperature (VPTT) of the nanocomposite hydrogels was conveniently unaltered versus that of the pure PNIPAAm hydrogel. Incorporation of nanoparticles caused enhancement in modulus as well as the extent and rate of deswelling. When cooled from 37 °C to 25 °C, mouse smooth muscle precursor cells (10T1/2) were effectively detached from nanocomposite hydrogel surfaces due to hydrogel swelling.

Keywords

Hydrogel; Thermoresponsive; Nanocomposite; Polysiloxane; Nanoparticle

1. INTRODUCTION

Thermoresponsive hydrogels reversibly switch from a water-swollen to a deswollen state in response to a temperature change.[1] They are produced via formation of crosslinked networks based on polymers which exhibit a lower critical solubility temperature (LCST) such as poly(*N*-isopropylacrylamide) (PNIPAAm) (LCST, ~32 °C).[1–3] Crosslinked PNIPAAm hydrogels exhibit a reversible volume phase transition in water from a swollen, hydrophilic state to a deswollen, relatively hydrophobic state when heated above its volume phase transition temperature (VPTT, ~33–35 °C).[4–6] Their thermoresponsive behavior has been studied for microfluidic actuation,[7–10] separation,[7, 11–12] controlled drug delivery[7, 13–15] and controlled detachment of adsorbed cells and proteins for applications such as cell sheet

*Author to whom correspondence should be addressed..

tissue engineering,[7, 16–17] anti-fouling coatings[18–20] and "self-cleaning" membranes for implanted biosensors.[21–24]

Enhancing the efficiency and expanding the utility of PNIPAAm in the aforementioned applications may require improvement in properties exhibited by conventional PNIPAAm hydrogels prepared via copolymerization of *N*-isopropylacrylamide (NIPAAm) and a bifunctional crosslinker such as *N*, *N*′-methylenebisacrylamide (BIS). Specifically, these properties may include deswelling/reswelling kinetics, mechanical properties and/or optical properties. Several design strategies to enhance the response rate of PNIPAAm hydrogels have been studied, including: comb-type networks,[25–27] heterogeneous morphologies,[28–31] poration,[32–35] or open channel structures[36] and inclusion of PNIPAAm nanoparticles[37] or discrete fillers.[38–41] However, in addition to the complexity of some of the aforementioned routes, the enhancement in deswelling-reswelling may produce diminished mechanical and/or optical properties. For instance, PNIPAAm hydrogels which are highly porous or exhibit a heterogeneous morphology are typically associated with reduced mechanical properties (e.g., modulus and strength) as a result of increased water content in the swollen state.[42–43] The turbidity of PNIPAAm hydrogels is also increased with a heterogeneous morphology as well as with the inclusion of certain fillers.[41–42, 44–45]

In this present work, we sought to design a PNIPAAm hydrogel system which maintains the VPTT of pure PNIPAAm hydrogel but enhances deswelling/reswelling kinetics as well as mechanical properties without significant loss of optical clarity. Thus, thermoresponsive nanocomposite hydrogels were prepared consisting of a PNIPAAm matrix and variable levels of colloidal polysiloxane nanoparticles (54 nm ave. diameter). The polysiloxane nanoparticles were prepared via anionic emulsion polymerization of octamethylcyclotetrasiloxane (D_4) and 1,3,5,7-tetramethyl-1,3,5,7-tetravinylcyclotetrasiloxane (D_4^{Vi}). The resulting nanoparticles were subsequently stabilized by free radical crosslinking the copoly(dimethylsiloxane/methylvinylsiloxane) chains inside the nanoparticles. The nanocomposite hydrogels were formed by photopolymerization (~7 °C) of aqueous solutions of NIPAAm, BIS and variable levels of polysiloxane nanoparticles (0.5–4 wt%). The effect of polysiloxane nanoparticle concentration on VPTT, optical clarity, morphology, deswelling/reswelling kinetics, mechanical properties and cell-release properties is presented.

2. MATERIALS AND METHODS

2.1. Materials

Octamethylcyclotetrasiloxane (D_4) and 1,3,5,7-tetramethyl-1,3,5,7-tetravinylcyclotetrasiloxane (D_4^{Vi}) were purchased from Gelest Inc. Brij 35, Brij 78, Tergitol solution (70% in H_2O), potassium hydroxide (KOH), potassium persulfate ($K_2S_2O_8$) and *N*-isopropylacrylamide (NIPAAm, 97%) were purchased from Aldrich. *N*, *N*′-methylenebisacrylamide (BIS, 99%) was obtained from Acros Organics. 1-[4-(2-Hydroxyethoxy)phenyl]-2-hydroxy-2-methyl-1-propane-1-one (Irgacure® 2959) was obtained from Ciba. Acetic acid was received from Fisher Scientific. All reagents were used as received. Mouse smooth muscle precursor cells (10T1/2) were obtained from American Type Culture Collection (ATCC).

2.2. Preparation of Crosslinked Polysiloxane Colloidal Nanoparticles

Polysiloxane colloidal particles were prepared by emulsion polymerization of D_4 and D_4^{Vi} (Fig. 1). In a 500 mL water-jacketed polymerization vessel equipped with a mechanical stirrer and Teflon stirring paddle, reflux condenser, and addition funnel was dissolved Brij 35 [$C_{12}H_{25}(OCH_2CH_2)_{23}OH$, 3.0 g, 2.5 mmol], Brij 78 [$C_{18}H_{37}(OCH_2CH_2)_{20}OH$; 6.75 g,

5.9 mmol) and Tergitol NP-40 [$C_9H_{19}Ph$-$(OCH_2CH_2)_{40}OH$; 5.35 g, 2.7 mmol) were dissolved in deionized (DI) water (147.0 g). A mixture of D_4 (31.2 g, 105.2 mmol) and D_4^{Vi} (7.8 g, 22.6 mmol) was added dropwise via the addition funnel to the aqueous solution with constant stirring (300 rpm). Then, 5 g of an aqueous solution of KOH (25 wt%) was added dropwise via the addition funnel. The resulting stable emulsion was then heated to 80 °C for 24 h with constant stirring (450 rpm). The final emulsion was cooled, filtered through a 10 μm filter bag, and the pH adjusted to 7 with aqueous acetic acid (25 wt%). The solid content of the emulsion was determined by weight loss from an aliquot after drying (115 °C, 8 h). Emulsion solid content: 26.5% (98.5% conversion).

Linear copoly(dimethylsiloxane/methylvinylsiloxane) was isolated from the aforementioned colloidal nanoparticles for subsequent characterization. A portion of the final emulsion was precipitated into ethanol, centrifuged and the isolated clear oil dried under vacuum. ^{1}H NMR (300 MHz; $CDCl_3$, δ_H): 0.1 (bs, Si–CH_3), 5.7–6.0 (m, Si–CH=CH_2); ratio of 10.1. Gel permeation chromatography (GPC): M_w/M_n = 47,100/16,500 g/mol, PDI = 2.85.

The colloidal nanoparticles were subsequently stabilized by crosslinking of the copoly(dimethylsiloxane/methylvinylsiloxane) chains within the nanoparticles via their vinyl groups (Fig. 1). The above final emulsion (50 g) was added to a 3-neck round bottom (rb) flask equipped with a Teflon-covered stir bar, reflux condenser, and nitrogen (N_2) inlet. After the addition of $K_2S_2O_8$ (0.5 g), the mixture was reacted at 80 °C for 10 h under N_2. The emulsion was cooled and filtered through a 10 μm filter bag. The resulting colloidal nanoparticles were purified via dialysis (Slide-A-Lyzer® Dialysis Cassette, MWCO = 10,000, Pierce Chemical Co.) against daily changes of DI water for 3 days. Emulsion solid content: 10.4%. Dynamic light scattering (DLS): 54 nm (average diameter) and 0.2 (polydispersity, PD) with particles ranging in size from 40 to 200 nm.

2.3. Characterization of Polysiloxane Colloidal Nanoparticles

Particle size of colloidal nanoparticles was determined by dynamic light scattering (DLS) (Brookhaven Instruments) with a detection angle of 90°. Measurements were carried out at 25 °C. An aliquot of the designated emulsion was highly diluted with DI water just prior to measurement in order to rule out interaction and multiple scattering effects. Cryogenic transmission electron microscopy (Cryo-TEM) was used to visualize the nanoparticles and confirm their lack of aggregation in water. A FEI-Q20 TEM, operated at 120 kV and equipped with a Gatan 626 cryo holder, was used for imaging. Further details on sample preparation and imaging analysis were previously described.[46]

2.4. Preparation of Nanocomposite Hydrogels

Nanocomposite hydrogels were prepared by *in situ* photopolymerization of aqueous precursor solutions containing NIPAAm monomer, BIS crosslinker, Irgacure-2959 photoinitiator, and crosslinked polysiloxane nanoparticles (Fig. 1, Table I). In a 50 mL rb flask equipped with a Teflon-covered stir bar, NIPAAm (1.0 g, 8.84 mmol), BIS (0.02 g, 0.13 mmol), and Irgacure-2959 (0.08 g, 0.36 mmol) were dissolved in DI water (the total volume equal to 7 mL including the volume of water introduced later by the nanoparticle emulsion) and the solution stirred under N_2 for 15 min. Finally, the appropriate amount of emulsion containing crosslinked colloidal nanoparticles was added and the mixture stirred for 10 min under N_2. In total, four different hydrogel compositions were prepared with varying amounts of colloidal nanoparticles:

- **a.** pure NIPAAm (no nanoparticles; a control),
- **b.** 0.5 wt%,

c. 1.0 wt%,

d. 2.0 wt%,

e. 3.0 wt%, and

f. 4.0 wt%

(wt% solids of nanoparticles with respect to NIPAAm weight).

Hydrogel sheets (1.5 or 0.5 mm thick) were prepared by first pipetting a precursor solution between two clamped glass microscope slides (75 × 50 mm) separated by polycarbonate spacers of appropriate thickness (1.5 mm for mechanical test and 0.5 mm for cell release test). The mold was submerged in an ice water bath (~7 °C) and exposed to longwave UV light (UV-Transilluminator, 6 mW/cm^2, 365 nm) for 30 min. After removal from the mold, hydrogel sheet was rinsed with DI water and then soaked in DI water for 2 days with daily water changes to remove impurities. Hydrogel sheets (1.5 mm thick) were used to prepare samples for morphological, VPTT, swelling, mechanical, and contact angle studies. Hydrogel sheets (0.5 mm thick) were used for cell-release studies.

2.5. Extent of Crosslinking

The amount of uncrosslinked material in select hydrogels was determined by weight loss following Soxhlet extraction. For a given hydrogel, three hydrogel discs (13 mm diameter, 1.5 mm thickness) were punched from a single hydrogel sheet with a die and immediately dried in a vacuum oven (30 in. Hg, 60 °C, 24 h) and weighed. The dried discs were extracted with dichloromethane in a Soxhlet apparatus for 12 h and weighed after similarly drying in a vacuum oven. The percentage of uncrosslinked material was calculated as the average weight difference of the extracted versus unextracted weight divided by the unextracted weight.

2.6. Morphology

The morphology of hydrogels was studied by scanning electron microscopy (SEM). The swollen hydrogel specimens were exposed to liquid nitrogen for 1 min and subsequently dried in lyophilizer (Labconco CentriVap Gel Dryer System) overnight. Cross-sections of the freeze-dried gels were subjected to Pt-sputter coating and viewed with a field emission SEM (FEI Quanta 600) at accelerated electron energy of 5–15 keV.

2.7. Volume Phase Transition Temperature (VPTT)

VPTT of swollen hydrogels were determined by differential scanning calorimetry (DSC, TA Instruments Q100). Water-swollen hydrogels were blotted with filter paper and a small piece sealed in a hermetic pan. After cooling to −50 °C, the temperature was increased to 50 °C at a rate of 3 °C/min for 2 cycles. The resulting endothermic phase transition peak is characterized by the initial temperature at which the endotherm starts (T_o), the peak temperature of the endootherm (T_{max}) and the enthalpy change (ΔH) of the phase transition. Data reported is from the 2nd cycle.

2.8. Deswelling Kinetics

Three hydrogel discs (13 mm diameter) were punched from a single sheet with a die. Water retention (WR) is defined as: $WR = (W_t - W_d)/W_s$. Each disc was sealed inside a vial containing 20 mL DI water, immersed in water bath for 24 h at 22 °C to achieve equilibrium (W_s) and quickly transferred into a 50 °C water bath. At 10, 20, 40, and 80 min, each disc was removed, blotted with a Kimwipe to remove surface water, immediately weighed (W_t)

and returned to the vial for subsequent measurements. After 80 min, the discs were dried in a vacuum oven (30 in. Hg, 60 °C, 24 h) and weighed (W_d).

2.9. Reswelling Kinetics

The kinetic reswelling ratio is defined as: $rSR = (W_t - W_d)/W_d$. The aforementioned previously dried discs (W_d) were each placed inside a sealed vial containing 20 mL DI water and immersed in a water bath at 22 °C. At 10, 20, 40, 80, 120, 200, 320 and 450 min, the samples were removed from the water bath and the masses were recorded as above (W_t).

2.10. Dynamic Mechanical Analysis (DMA)

DMA of hydrogels were measured in the compression mode with a dynamic mechanical analyzer (TA Instruments Q800) equipped with parallel-plate compression clamp with a diameter of 40 mm (bottom) and 15 mm (top). Swollen hydrogel discs of constant dimension (13 mm diameter, 1.5 mm thickness) were punched from a hydrogel sheet and clamped between the parallel plates. Silicone oil was then placed around the exposed edges of the hydrogel to prevent dehydration. Following equilibration at the 25 °C (5 min), the samples were tested in a multi-frequency-strain mode (1 to 25 Hz) at the temperature of 25 °C (below the VPTT). Results reported are based on the average of five individual specimens.

2.11. Temperature-Dependent Cell Release

Hydrogel sheets (**a–f**) were prepared as above under sterile conditions. A “PEO-RGDS” hydrogel was prepared from poly(ethylene oxide)-diacrylate (PEO-DA, M_n = 6000 g/mol) containing the acrylate-derivatized cell adhesion peptide RGDS (acryoyl-PEO-RGDS) using standard procedures.[47] Photoinitiator solution (10 μL of 30 wt% solution of DMAP in NVP) was added for every one mL of aqueous solution containing 10 wt% PEO-DA macromers and 1 μmol/mL acryoyl-PEO-RGDS in PBS. The PEO-DA and PNIPAAm-based precursor solutions were each cured between two glass sheets separated by 0.5 mm polycarbonate spacers by exposure to 365 nm UV light (UV-Transilluminator, 6 mW/cm^2) for 2 min. All hydrogel formulations were permitted to swell for two days in phosphate-buffered saline (PBS; pH = 7.4) with daily PBS changes to remove hydrogel impurities. Swollen hydrogel discs of constant dimension (9 mm diameter, 0.5 mm thickness) were punched from each hydrogel sheet and transferred to a 24 well plate containing media in each well. The plate was then incubated at 37 °C (above VPTT) for 2 h. Mouse smooth muscle precursor cells (10T1/2) were seeded onto each hydrogel surfaces at 25,000 cells/cm^2. After incubation at 37 °C for 4 h, the 24 well plate was transferred to a Zeiss Axiovert A200 microscope and air-cooled to 25 °C (below VPTT) at a rate of ~2 °C/min thereby causing **a–f** to swell. The media within each well containing the hydrogel disc provided water for the swelling process. The well plate was then transferred back to a 37 °C incubator for 4 h and a second cooling cycle was similarly performed. For each cooling cycle, images were captured at two second intervals.

3. RESULTS AND DISCUSSION

3.1. Preparation of Crosslinked Polysiloxane Colloidal Nanoparticles

Polysiloxane colloidal nanoparticles were prepared by anionic ring-opening emulsion polymerization of D_4 and D_4^{Vi} and subsequent crosslinking (Fig. 1).[48] The colloidal nanoparticles were internally crosslinked via free radical reaction of the vinyl groups. Surfactant and other reaction impurities were removed from the resultant emulsion via dialysis. This process yielded stable polysiloxane colloidal nanoparticles having an average diameter of 54 nm (PD = 0.2).

3.2. Preparation of Nanocomposite Hydrogels: Crosslinking, Transparency and Morphology

Nanocomposite hydrogels (**b–f**) were formed by UV-cure at ~7 °C for 30 min (Fig. 1, Table I). UV-cure is advantageous versus free radical cure crosslinking[6, 49–50] as it involves shorter times and can be done at lower temperatures.[51–53] The efficacy of UV-cure was confirmed by Soxhlet extraction (CH_2Cl_2, 12 hr) of hydrogels containing 4 wt% nanoparticles (**f**) and pure PNIPAAm hydrogel (**a**) which both exhibited no detectable weight loss (<0.1 wt%). Nanocomposite hydrogels gradually became less transparent with higher polysiloxane nanoparticle content. However, hydrogels (**b–f**), prepared with 54 nm (ave. diam.) nanoparticles, were significantly more transparent than those prepared with lower amounts of analogous 219 nm (ave. diam.) polysiloxane nanoparticles (**g**).[54]

UV-cure was conducted at a preparation temperature (T_{prep}) of <20 °C in order to achieve a homogeneous PNIPAAm hydrogel morphology which is associated with transparency and enhanced mechanical properties.[42–45] In contrast, a T_{prep} > 20 °C produces a heterogeneous PNI-PAAm hydrogel which display enhanced swelling but are opaque and mechanical weaker. The homogeneity of the PNIPAAm hydrogel matrix was confirmed by the optical transparency of the PNIPAAm hydrogel (**a**, no nanoparticles). SEM imaging of lyopholized hydrogels was used to assess their morphology.[55] Hydrogels **a–f** all exhibited a similar homogeneous morphology characterized by a uniform porous structure (Fig. 2).

3.3. Volume Phase Transition Temperature (VPTT)

During the volume phase transition, PNIPAAm hydrogels exhibit an endothermic peak due to breaking of hydrogen bonds of surrounding water molecules.[56–57] The peak is detectable by DSC and the may be designated by the peak's onset (T_o) or maximum temperature (T_{max}).[53, 58–59] The DSC thermograms of swollen samples of **a–f** were used to determine VPTT (Fig. 3, Table I). T_o values were determined from the intersecting point between two tangent lines from the baseline and slope of the endothermic peak.[58] Polysiloxane nanoparticles did not produce a significant change in the VPTT (T_o) of nanocomposite hydrogels (**b–f**) compared to that of a pure PNIPAAm hydrogel (**a**). This was similarly observed for nanocomposite prepared with larger polysiloxane nanoparticles.[41] Because of their discrete nature, nanoparticles apparently do not interfere with the dissociation of water molecules from hydrophobic groups when heated above the VPTT.

3.4. Deswelling and Reswelling Kinetics

Nanocomposite hydrogels containing 3 and 4 wt% nanoparticles (**e** and **f**, respectively) exhibited a dramatic enhancement in both the rate and extent of deswelling compared to the pure hydrogel (**a**) and as well as that containing larger polysiloxane nanoparticles (**g**) (Fig. 4). Within only ~40 min at 50 °C, WR of **e** and **f** reached equilibrium and the final WR of **f** is nearly 70% lower than that of **e**. Because the morphology of the nanocomposite hydrogels did not change significantly with nanoparticle content, we suggest that the hydrophobic nature of the polysiloxane particles facilitates the rapid removal of water from the hydrogel upon heating above the VPTT. Reswelling equilibrium was achieved more quickly for nanocomposite hydrogels (**b–g**) versus the pure hydrogel (**a**). The final rSR systematically decreased with nanoparticle content and may be attributed to their hydrophobic nature which reduces total water uptake.

3.5. DMA

To maintain their swollen state, silicone oil was placed around the hydrogel disc during DMA. Storage modulus (G′) is related to a materials stiffness or resistance to deformation.[60] G′ of the nanocomposite hydrogels (**b–f**) increased with higher levels of polysiloxane

nanoparticles (Fig. 5). Hydrogel modulus is directly influenced by its swelling such that routes to enhance stiffness and strength often rely on reduction of swelling.[43] Thus, the relative differences the G′ of **b–f** can be related to their swelling (i.e., rSR at 450 min, Fig. 4). With increased levels of 54 nm nanoparticles, swelling is reduced which contributed to an increase in G'. Interestingly, despite higher swelling, the nanocomposite hydrogel containing larger nanoparticles (1 wt% 219 nm; **g**) exhibited higher G′ values versus that of **b–f**. While **g** and **c** both contained 1 wt% nanoparticles, **c** contains a higher number of nanoparticles with a higher nanoparticle surface area. Given the relatively lower G′ of **c**, it suggests that the nanoparticles due not form a strong interface with the hydrogel matrix so as to have a reinforcing effect.

3.6. Temperature-Dependent Cell Release Behavior

On the basis of their change to a round cell morphology, PNIPAAm-based hydrogels (**a–f**) cooled from 37 °C (above VPTT) to 25 °C (below VPTT) caused the release of 10T1/2 cells due to hydrogel swelling (Fig. 6). In contrast, cells cultured on the cell-adhesive, non-thermoresponsive PEO-RGDS hydrogel[61] maintained an extended morphology indicative of cell adhesion and spreading. It was observed that more cells adhered to the nanocomposite hydrogels (**b–f**) compared to the pure PNI-PAAm hydrogel (**a**) which may be explained by the higher hydrophobicity of **b–f** which promotes protein and cell adhesion.[62–64] After the first cooling cycle, a round cell morphology indicative of end stages of cell detachment was observed for cells on **a–f**. Following a subsequent second heating-cooling cycle, the round morphology was even more pronounced on **a–f** (Fig. 6).

4. CONCLUSIONS

Thermoresponsive nanocomposite hydrogels comprised of a PNIPAAm hydrogel matrix and polysiloxane colloidal nanoparticles (54 nm ave. diameter) were prepared via *in situ* photopolymerization of aqueous solutions of NIPAAm monomer, BIS crosslinker, photoinitiator and 0.5–4.0 wt% polysiloxane nanoparticles (wt% solids of nanoparticles with respect to NIPAAm weight) at ~7 °C. The convenient VPTT of PNIPAAm hydrogels was maintained due to the discrete, chemically independent nature of the embedded polysiloxane nanoparticles. SEM analysis confirmed their homogeneous morphology due to the low preparation temperature. The optical clarity of the nanocomposite hydrogels prepared with ~54 nm nanoparticles progressively decreased with higher nanoparticle concentration. However, their optical clarity was greater than that of nanocomposite membranes prepared with 219 nm polysiloxane nanoparticles. Increasing the nanoparticle content led to an increase in storage modulus (G′) as well as an enhanced rate and extent of deswelling. When cooled from 37 °C to 25 °C, mouse smooth muscle precursor (10T1/2) cells were shown to effectively detach from nanocomposite hydrogel surfaces. Thus, this design permits simultaneous improvement in PNIPAAm hydrogel deswelling kinetics, mechanical properties and optical properties.

Acknowledgments

Funding from NIH/NIDDK (1R21DK082930-01A1) and NSF/CBET (0854462) is gratefully acknowledged.

References and Notes

1. Wu, XY.; Zhang, Q.; Arshady, R. Stimuli sensitive hydrogels, The PBM Series: Introduction to Polymeric Biomaterials. Arshady, R., editor. Vol. Vol. 1. London: Citrus Books; 2003. p. 162-163.
2. Heskins M, Guillet JE. Solution properties of poly(*N*-isopropylacrylamide). J. Macromol. Sci. Chem. Part A. 1968; 2:1441.

3. Schild HG. Poly(*N*-isopropylacrylamide): Experiment, theory, and application. Prog. Polym. Sci. 1992; 17:163.
4. Hirokawa Y, Tanaka T. Volume phase transition in a nonionic gel. J. Chem. Phys. 1984; 81:9379.
5. Hoffman AS, Afrassiabi A, Dong LC. Thermally reversible hydrogels: II. Delivery and selective removal of substances from aqueous solution. J. Controlled Release. 1986; 4:213.
6. Zhang J, Pelton R, Deng Y. Temperature-dependent contact angles of water on poly(*N*-isopropylacrylamide) gels. Langmuir. 1995; 11:2301.
7. Kumar A, Srivastava A, Galaev IY, Mattiasson B. Smart polymers: Physical forms and bioengineering applications. Prog. Polym. Sci. 2007; 32:1205.
8. Eddington DT, Beebe DJ. Flow control with hydrogels. Adv. Drug Deliv. Rev. 2004; 56:199. [PubMed: 14741116]
9. Harmon ME, Tang M, Frank CW. A microfluidic actuator based on thermoresponsive hydrogels. Polymer. 2003; 44:4547.
10. Li Z, He Q, Ma D, Chen H. On-chip integrated multi-thermo-actuated microvalves of poly(*N*-isopropylacrylamide) for microflow injection analysis. Anal. Chimica Acta. 2010; 665:107.
11. Zhiming L, Qiaohong H, Dan M, Hengwu C, SS A. Thermoswitchable electrokinetic ion-enrichment/elution based on a poly(*N*-isopropylacrylamide) hydrogel plug in a microchannel. Anal. Chem. 2010; 82:10030. [PubMed: 21105674]
12. Freitas RFS, Cussler EL. Temperature sensitive gels as size selective absorbents. Sep. Sci. Tech. 1987; 22:911.
13. Qiu Y, Park K. Environment-sensitive hydrogels for drug delivery. Adv. Drug Deliv. Rev. 2001; 53:321. [PubMed: 11744175]
14. Chilkoti A, Dreher MR, Meyer DE, Raucher D. Targeted drug delivery by thermally responsive polymers. Adv. Drug Deliv. Rev. 2002; 54:613. [PubMed: 12204595]
15. Nakayama M. Thermoresponsive polymeric materials for drug delivery systems. Drug Delivery Sys. 2008; 23:627.
16. Yamato M, Akiyama Y, Kobayashi J, Yang J, Kikuchi A, Okano T. Temperature-responsive cell culture surfaces for regenerative medicine with cell sheet engineering. Prog. Polym. Sci. 2007; 32:1123.
17. Kobayashi J, Okano T. Fabrication of a thermoresponsive cell culture dish: A key technology for cell sheet tissue engineering. Sci. Tech. Adv. Mater. 2010; 11:1.
18. Callwaert M, Rouxhet PG, Boulange-Petermann L. Modifying stainless steel surfaces with responsive polymers: Effect of PSPAA and PNIPAAM on cell adheshion and oil removal. J. Adhesion. Sci. Technol. 2005; 19:765.
19. Cunliffe D, Smart CA, Tsibouklis J, Young S, Alexander C, Vulfson EN. Bacterial adsorption to thermoresponsive polymer surfaces. Biotechnol. Lett. 2000; 22:141.
20. Ista L, Lopez G. Lower critical solubility temperature materials as biofouling release agents. J. Indust. Mircrobiol. Biotechnol. 1998; 20:121.
21. Chen J, Yoshida M, Maekawa Y, Tsubokawa N. Temperature-switchable vapor sensor materials based on *N*-isopropylacrylamide and calcium chloride. Polymer. 2001; 42:9361.
22. Guenther M, Gerlach G, Kuckling D, Kretschmer K, Corten C, Weber J, Sorber J, Suchaneck G, Arndt K-F. Chemical sensors based on temperature-responsive hydrogels. Proc. SPIE Int. Soc. Opt. Eng. 2006; 6167:61670T/1.
23. Gant R, Hou Y, Grunlan MA, Cote GL. Development of a self-cleaning sensor membrane for implantable biosensors. J. Biomed. Mater. Res. 2009; 90A:695.
24. Gant R, Abraham A, Hou Y, Grunlan MA, Cote GL. Design of a self-cleaning thermoresponsive nanocomposite hydrogel membrane for implantable biosensors. Acta Biomaterialia. 2010; 6:2903. [PubMed: 20123136]
25. Liu Q, Zhang P, Qing A, Lan Y, Shi J, Lu M. Synthesis of rapid responsive gels comprising hydrophilic backbone and poly(*N*-isopropylacrylamide) graft chains by RAFT polymerization and end-linking processes. Polymer. 2006; 47:6963.
26. Matsuura T, Sugiyama M, Annaka M, Hara Y, Okano T. Microscopic implications of rapid shrinking of comb-type grafted poly(*N*-isopropylacrylamide) hydrogels. Polymer. 2003; 44:4405.

27. Yoshida R, Uchida K, Kaneko Y, Sakai K, Kikuchi A, Sakurai Y, Okano T. Comb-type grafted hydrogels with rapid de-swelling response to temperature changes. Nature. 1995; 374:240.
28. Zhang X-H, Yang Y-Y, Chung T-S. The influence of cold treatment on the properties of temeprature-sensitive poly(*N*isopropylacrylamide) hydrogels. J. Coll. Interface Sci. 2002; 246:105.
29. Xue W, Champ S, Huglin MB, Jones TGJ. Rapid swelling and deswelling in cryogels of crosslinked poly(*N*-isopropylacrylamide-co-acrylic). Europ. Polym. J. 2004; 40:703.
30. Yan Q, Hoffman AS. Synthesis of macroporous hydrogels with rapid swelling and deswelling properties for delivery of macromolecules. Polymer. 1995; 36:887.
31. Zhang X-Z, Yang Y-Y, Chung T-S. Effect of mixed solvents on characteristics of poly(*N*-isopropylacrylamide) gels. Langmuir. 2002; 18:2538.
32. Serizawa T, Uemura M, Kaneko T, Akashi M. Rapid and controlled deswelling of porous poly(*N*-isopropylacrylamide) hydrogels prepared by the templating of interpenetrated nanoporous silica particles. J. Polym. Sci., Part A: Polym. Chem. 2002; 40:3542.
33. Serizawa T, Wakita K, Akashi M. Rapid deswelling of porous poly(*N*-isopropylacrylamide) hydrogels prepared by incorporation of silica particles. Macromolecules. 2002; 35:10.
34. Serizawa T, Wakita K, Kaneko T, Akashi M. Thermore-sponsive properties of porous poly(*N*-isopropylacrylamide) hydrogels prepared in the presence of nanosized silica particles and subsequent acid treatment. J. Polym. Sci., Part A: Polym. Chem. 2002; 40:4228.
35. Zhang X-Z, Yang Y-Y, Chung T-S, Ma K-X. Preparation and characterization of fast response macroporous poly(*N*isopropylacrylamide) hydrogels. Langmuir. 2001; 17:6094.
36. Kaneko T, Asoh T-A, Akashi M. Ultrarapid molecular release from poly(*N*-isopropylacrylamide) hydrogels perforated using silica nanoparticle networks. Macromol. Chem. Phys. 2005; 206:566.
37. Zhang J-T, Huang S-W, Xue Y-N, Zhuo R-X. Poly(N-isopropylacrlamide) nanoparticle incorporated PNIPAAm hydrogels with fast shrinking kinetics. Macro. Rapid Comm. 2005; 26:1346.
38. Haraguchi K, Takehisa T. Nanocomposite hydrogels: A unique organic–inorganic network structure with extraordinary mechanical, optical and swelling/deswelling properties. Adv. Mater. 2002; 14:1120.
39. Zeng K, Wang L, Zheng S. Rapid deswelling and reswelling response of poly(*N*-isopropylacrylamide) hydrogels via formation of interpenetrating polymer networks with polyhedral oligomeric silsequioxane-capped poly(ethylene oxide) amphiphilic telechelics. J. Phys. Chem. B. 2009; 113:11831. [PubMed: 19670841]
40. Tan Y, Xu K, Wang P, Li W, Sun S, Dong LS. High mechanical strength and rapid response rate of poly(*N*-isopropylacrylamide) hydrogel crosslinked by starch-based nanospheres. Soft Matter. 6:1467. 201.
41. Hou Y, Matthews AR, Smitherman AM, Bulick AS, Hahn MS, Hou H, Han A, Grunlan MA. Thermoresponsive nanocomposite hydrogels with cell-releasing behavior. Biomaterials. 2008; 29:3175. [PubMed: 18455788]
42. Rathjen CM, Park C-H, Goodrich PR, Walgenbach DD. The effect of preparation temperature on some properties of a temperature-sensitive hydrogel. Polym. Gels Networks. 1995; 3:101.
43. Anseth KS, Bowman CN, Brannon-Peppas L. Mechanical properties of hydrogels and their experimental determination. Biomaterials. 1996; 17:1647. [PubMed: 8866026]
44. Ju S-J, Chu L-Y, Zhu Z-L, Hu L, Song H, Chen W-M. Effects of internal microstructures of poly(*N*-isopropylacrylamide) hydrogels on thermo-responsive volume phase-transition and controlled-release characteristics. Smart Mater. Struct. 2006; 15:1767.
45. Kayaman N, Kazan D, Erarslan A, Okay O, Baysal BM. Structure and protein separation efficiency of poly(*N*-isopropylacrylamide) gels: Effect of synthesis conditions. J. Appl. Polym. Sci. 1998; 67:805.
46. Abbas S, Li Z, Hassan H, Lodge TP. Thermoreversible morphology transitions of poly(styrene-*b*-dimethylsiloxane) diblock copolymer micelles in dilute solution. Macromolecules. 2007; 40:4048.
47. Hahn MS, Taite LJ, Moon JJ, Rowland MC, Ruffino KA, West JL. Photolithographic patterning of polyethylene glycol hydrogels. Biomaterials. 2006; 27:2519. [PubMed: 16375965]
48. Zhang D, Jiang X, Yang C. Microemulsion polymerization of siloxane with nonionic surfactants as emulsifiers. J. Appl. Polym. Sci. 2003; 89:3587.

49. Kato E, Kitada T, Nakamoto C. Anomalous compressibility of *N*-isopropylacrylamide gels near the volume phase transition temperature. Macromolecules. 1993; 26:1758.
50. Park TG, Hoffman AS. Deswelling characteristics of poly(*N*-isopropylacrylamide) hydrogels. J. Appl. Polym. Sci. 1994; 52:85.
51. Fisher JP, Dean D, Engel PS, Mikos AG. Photoinitiated polymerization of biomaterials. Annu. Rev. Mater. Res. 2001; 31:171.
52. Liang L, Feng Z, Peurrung L, Viswanathan V. Temperature-sensitive membranes prepared by UV photopolymeriztion of *N*-isopropylacrylamide on surfaces of porous hydrophilic polypropylene membranes. J. Membrane Sci. 1999; 162:235.
53. Singh D, Knuckling D, Choudhary V, Adler H-J, Koul V. Synthesis and characterization of poly(*N*-isopropylacrylamide) films by photopolymerization. Polym. Adv. Technol. 2006; 17:186.
54. Hou Y, Matthews AR, Smitherman AM, Bulick AS, Hahn MS, Grunlan MA. Thermoresponsive nanocomposite hydrogels with cell-releasing behavior. Biomaterials. 2008; 29:3175. [PubMed: 18455788]
55. Bekiari V, Lianos P. Photophysical behavior of terpyridine-lanthanide ion complexes incorporated in a poly(*N*,*N*-dimethylacrylamide) hydrogel. Langmuir. 2006; 22:8602. [PubMed: 16981782]
56. Shibayama M, Mizutani S-Y, Nomura S. Thermal properties of copolymer gels containing *N*-isopropylacrylamide. Macromolecules. 1996; 29:2019.
57. Shibayama M, Morimoto M, Nomura S. Phase separation induced mechanical transition of poly(*N*-isopropylacrylamide)/water isochore gels. Macromolecules. 1994; 27:5060.
58. Otake K, Inomata H, Konno M, Saito S. Thermal analysis of the volume phase transition with *N*-isopropylacrylamide gels. Macromolecules. 1990; 23:283.
59. Feil H, Bae YH, Feijen J, Kim SW. Effect of comonomer hydrophilicity and ionization on the lower critical solution temperature of *N*-isopropylacrylamide copolymers. Macromolecules. 1993; 26:2496.
60. Wicks, ZW.; Jones, FN.; Pappas, SP. Organic Coatings Science and Technology. 2nd edn. New York: John Wiley & Sons; 1999. p. 68-69.
61. Mann BK, Tsai AT, Scott-Burden T, West JL. Modification of surfaces with cell adhesion peptides alters extracellular matrix deposition. Biomaterials. 1999; 20:2281. [PubMed: 10614934]
62. Lee JH, Khang G, Lee JW, Lee HB. Interaction of different types of cells on polymer surfaces with wettability gradient. J. Colloid Interface Sci. 1998; 205:323. [PubMed: 9735195]
63. Tamada Y, Ikada Y. Effect of preadsorbed proteins on cell adhesion to polymer surfaces. J. Colloid Interface Sci. 1993; 155:334.
64. Tamada Y, Ikada Y. Cell adhesion to plasma-treated polymer surfaces. Polymer. 1993; 34:2208.

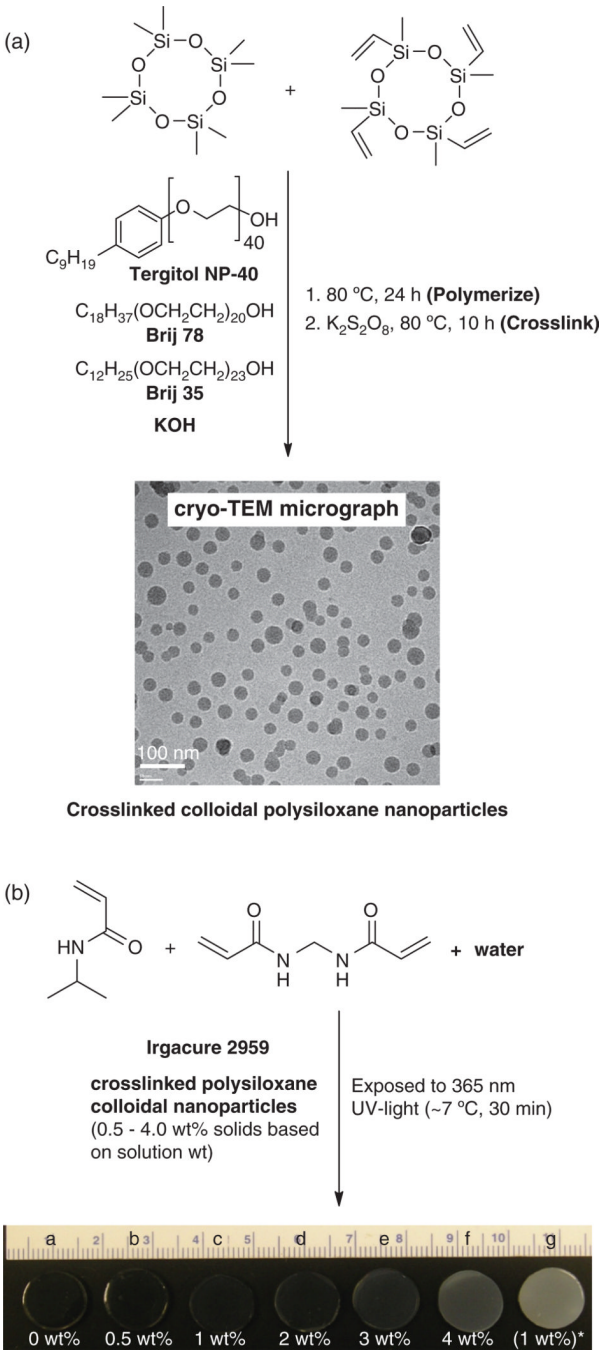

Fig. 1.

(a) Preparation of colloidal polysiloxane nanoparticles via emulsion polymerization and subsequent crosslinking and (b) preparation of thermoresponsive nanocomposite hydrogels with variable wt% nanoparticles. [“g”: prepared with 1 wt% polysiloxane nanoparticles, ave. diam. = 219 nm].

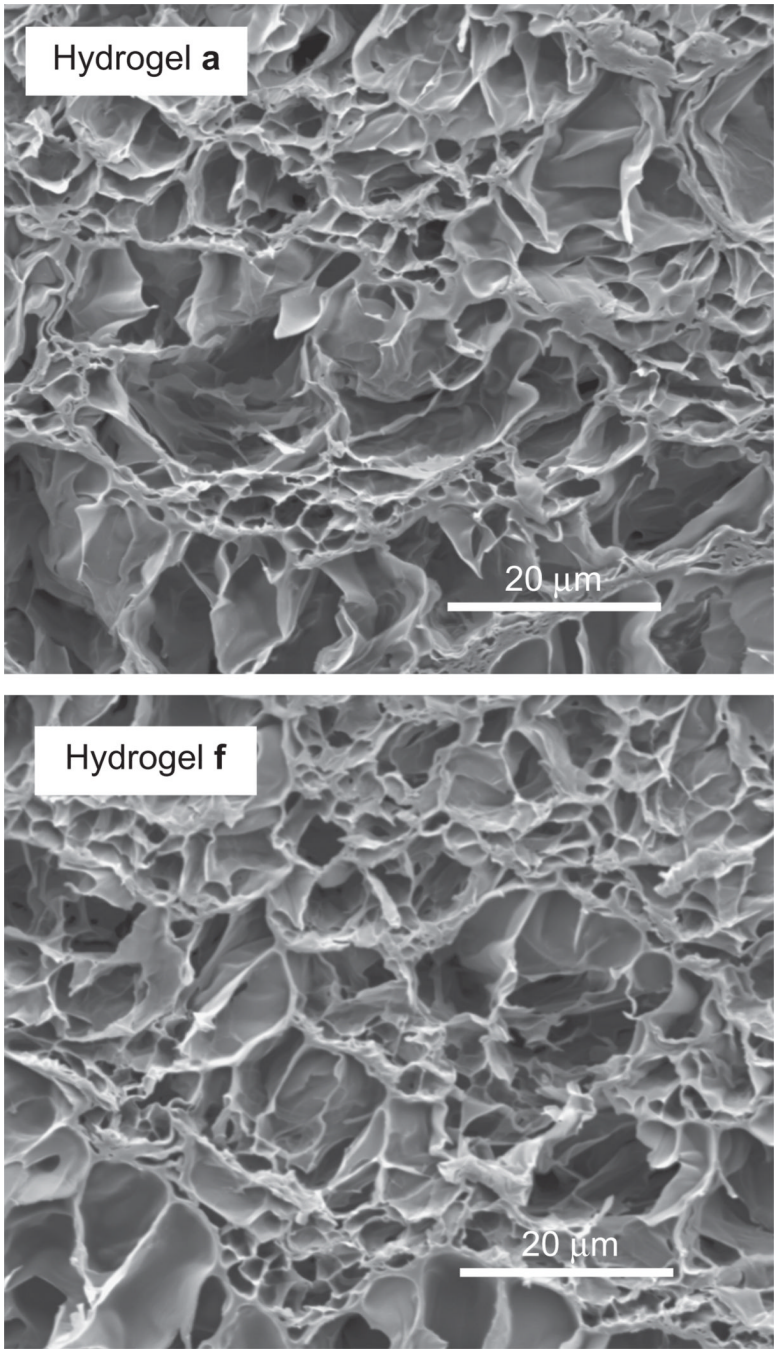

Fig. 2.
SEM micrographs of hydrogel **a** (0 wt% nanoparticles) and hydrogel **f** (4 wt% nanoparticles).

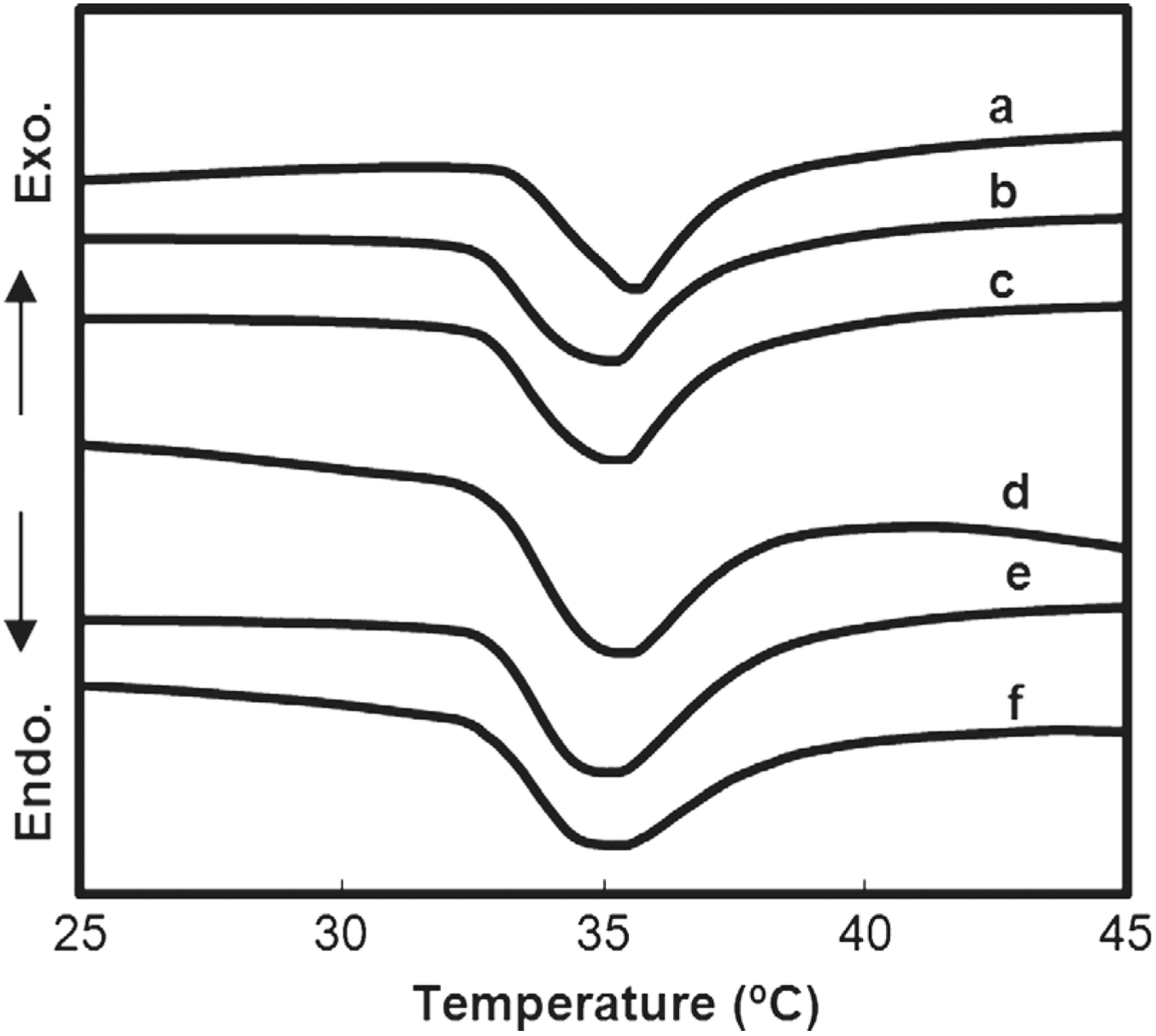

Fig. 3.
Measurement of VPTT by DSC.

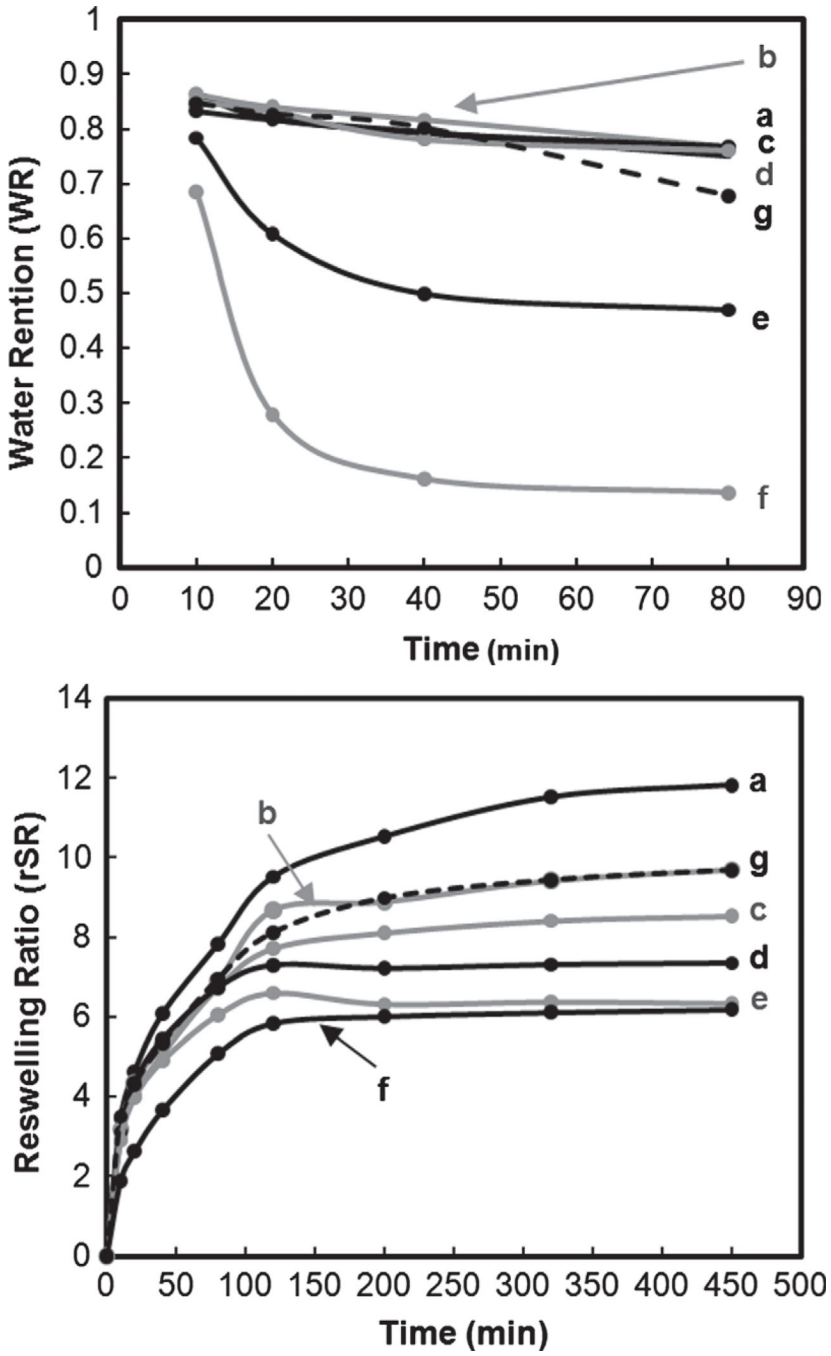

Fig. 4.
Deswelling (top) and reswelling (bottom) kinetics.

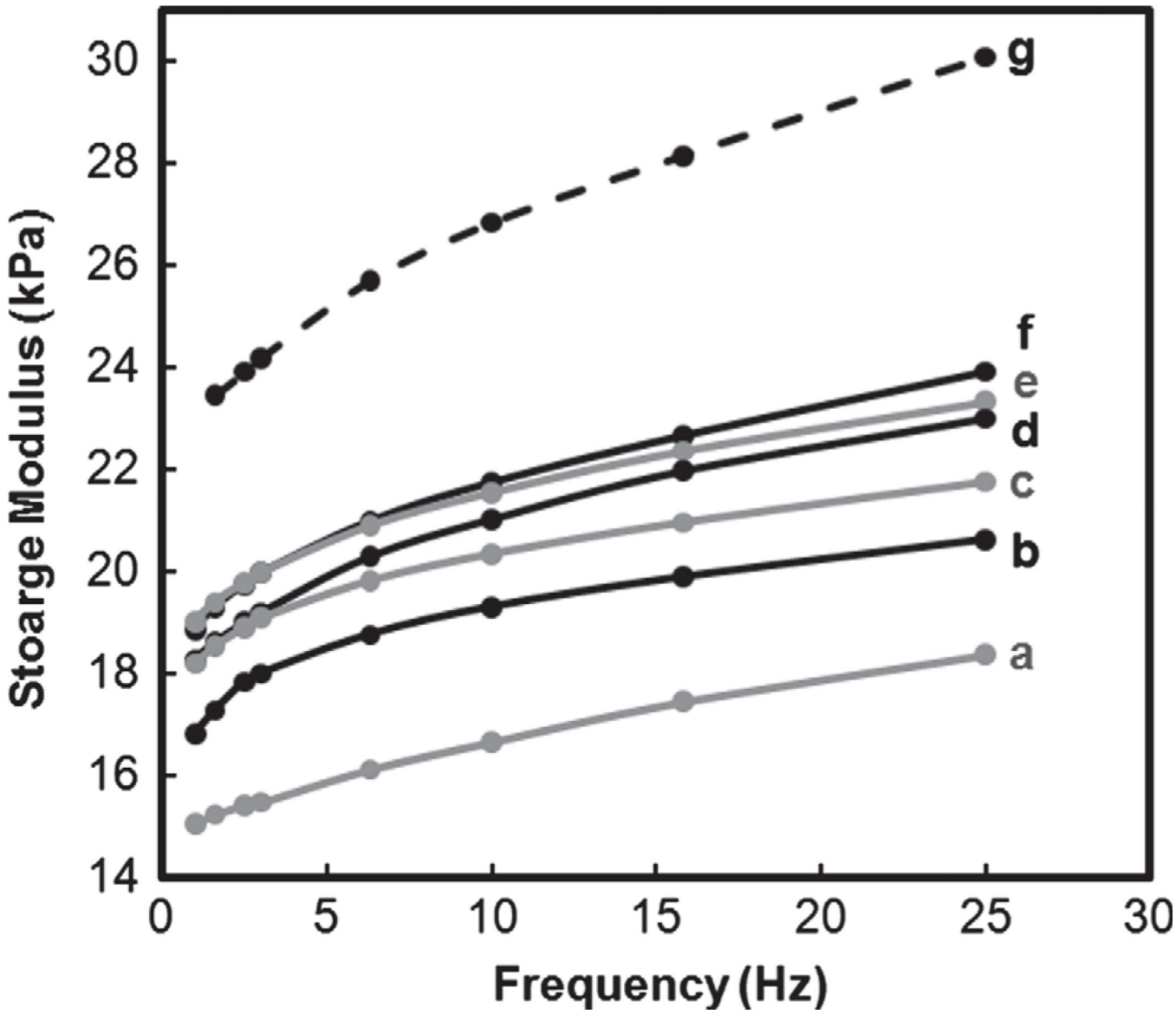

Fig. 5.
Storage moduli (G′) in compression.

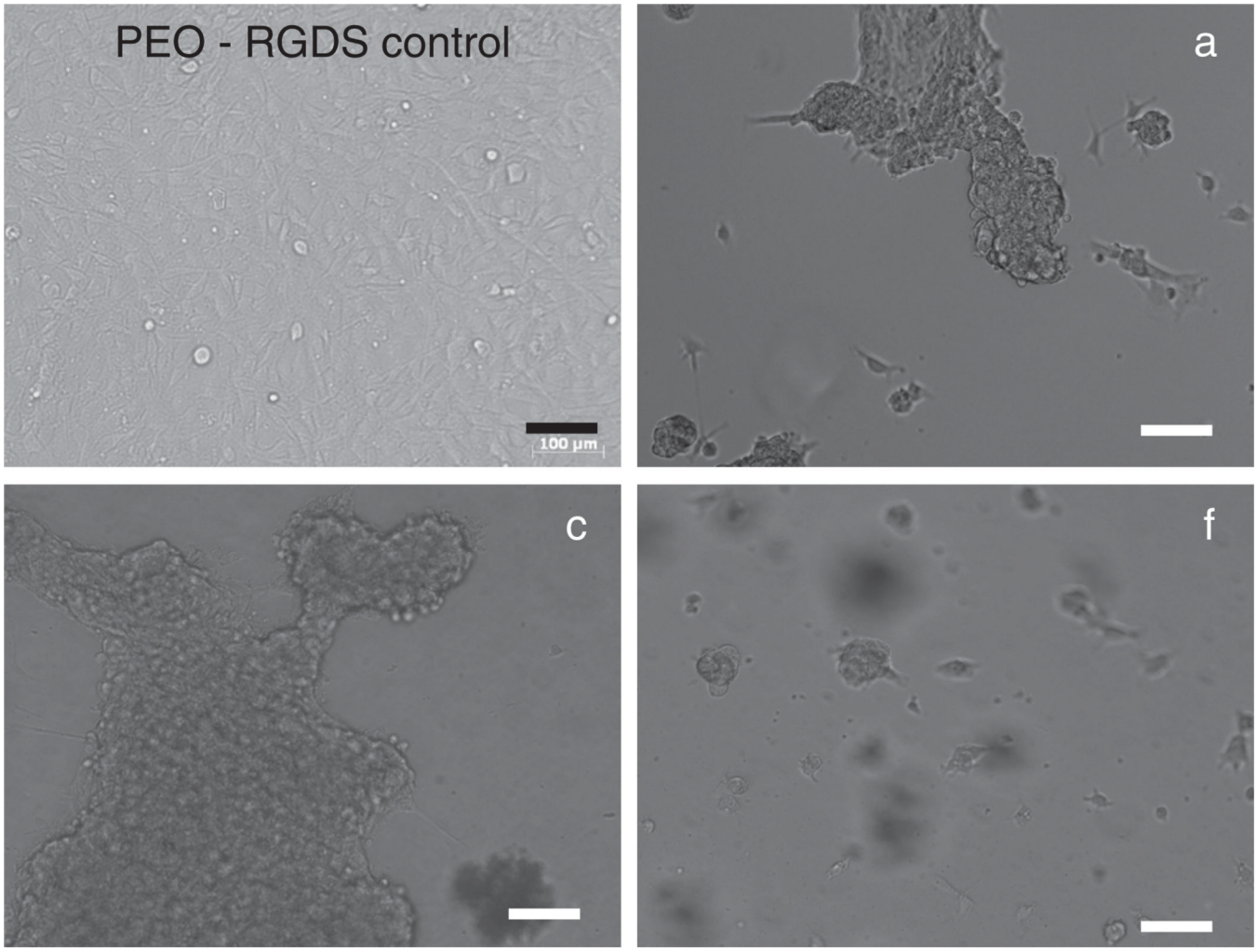

Fig. 6.

Mouse smooth muscle precursor (10T1/2) cells displayed a rounded morphology indicative of detachment on hydrogels a, c and f following two cycles of thermal cooling from 37 °C to 25 °C. A PEO-RGDS hydrogel served as a cell-adhesive but non-thermoresponsive control. All scale bars are 100 μm.

Table I

Composition, thermal transition properties and mechanical properties.

Composition		Volume phase transition temperature (VPTT)		
Hydrogel	Solid wt% nanoparticles	T_o (°C)	T_{max} (°C)	ΔH (J/g)
a	0	32.7	35.4	5.25
b	0.5	32.8	35.2	4.60
c	1.0	33.1	35.6	4.65
d	2.0	32.9	35.3	4.42
e	3.0	32.7	35.2	5.56
f	4.0	32.6	35.1	5.47